Current Cardiology Reports (2020) 22: 29
https://doi.org/10.1007/s11886-020-01281-6

REGENERATIVE MEDICINE (SM WU, SECTION EDITOR)

Cellular Reprogramming Approaches to Engineer Cardiac Pacemakers

Angel Xiao [1] · Hee Cheol Cho [2,3]

Published online: 30 March 2020

Abstract

Purpose of Review The goal of this paper is to review present knowledge regarding biological pacemakers created by somatic reprogramming as a platform for mechanistic and metabolic understanding of the rare subpopulation of pacemaker cells, with the ultimate goal of creating biological alternatives to electronic pacing devices.

Recent Findings Somatic reprogramming of cardiomyocytes by reexpression of embryonic transcription factor T-box 18 (TBX18) converts them into pacemaker-like. Recent studies take advantage of this model to gain insight into the electromechanical, metabolic, and architectural intricacies of the cardiac pacemaker cell across various models, including a surgical model of complete atrioventricular block (CAVB) in adult rats.

Summary The studies reviewed here reinforce the potential utility of TBX18-induced pacemaker myocytes (iPMS) as a minimally invasive treatment for heart block. Several challenges which must be overcome to develop a viable therapeutic intervention based on these observations are discussed.

Keywords Atrioventricular block · Induced pacemaker myocytes · Biological pacemaker · Gene therapy · Bradycardia

Introduction

The initiation of heart beats depends critically upon pacemaker cells, a subpopulation of < 10,000 cells within the ~ 10 billion myocyte and non-myocyte cells of the adult mammalian heart [1]. Failure of the native pacemaker cells of the sinoatrial node (SAN) to function results in bradycardias that could lead to syncope and circulatory collapse. Current therapy relies on costly electronic device–based cardiac pacing. In addition to a rising complication incidence due to indwelling hardware (lead fractures, infections, replacements), these devices have proven to be incompatible for pediatric patients who require a dynamic, adaptable solution to account for their growth [2–4].

Biological pacemakers have been developed as a minimally invasive alternative treatment modality. Specifically, we have demonstrated that the focal reexpression of an embryonic transcription factor T-box 18 (TBX18) could convert normally quiescent ventricular cardiomyocytes into induced pacemaker-like cells, recapitulating hallmark features of cells in the sinoatrial node (SAN) [2, 5–7]. To better understand the mechanistic basis of pacemaking by the induced pacemaker cells, there is a need for comprehensive tissue-level models as well as clinically relevant small animal models to successfully recapitulate the progression of chronic bradycardia [8–11] and evaluate disease-modifying activity of biological pacemakers.

This review aims to highlight ongoing investigations into the cellular and tissue-level characterization of the induced pacemaker cells. In addition, we review a novel small animal model of complete atrioventricular block (CAVB) which has potential to fast-track future treatment development and refinements. These studies elucidate the design principles of the native SAN that can be reverse-engineered for the goal of making therapeutically relevant tissue-engineered SA nodes (eSANs).

This article is part of the Topical Collection on *Regenerative Medicine*

✉ Hee Cheol Cho
heecheol.cho@emory.edu

Angel Xiao
axxiao@emory.edu

[1] Emory University School of Medicine, 201 Dowman Dr, Atlanta, GA 30322, USA

[2] Department of Pediatrics, Emory University, HSRB E-184, 1760 Haygood Drive, Atlanta, GA 30322, USA

[3] Department of Biomedical Engineering, Emory University, HSRB E-184, 1760 Haygood Drive, Atlanta, GA 30322, USA

Induced Pacemaker Myocytes Are Electrically Well-Insulated

In vitro functional assessment of engineered cardiac tissue constructs is complex and multifactorial [12, 13]. A functional, standardized readout capable of providing comparison across different models and laboratories could greatly guide optimization of the structure and function of derived tissues. The strength-duration relationship is presented as a potential tool to prioritize properties that govern the electrical excitability of cardiac myocytes. The negative correlation between the strength of a transmembrane current source with the threshold duration for excitation is classically described by the quasi-hyperbolic Lapicque-Hill equation [13, 14]. Beyond a benchmark of comparison, cell excitability testing of pacemaker cells can help define the parameters needed for successful electrical field pacing in vitro and physiological integration in vivo.

2D and 3D cultures of neonatal rate ventricular myocytes (NRVMs) and cardiac fibroblasts isolated from post-natal day 1–3 rats were employed as models of the ventricular myocardium. Strength-duration tests on these constructs discerned that smaller culture dimension, perpendicular anisotropic orientation of the cardiac tissue constructs with respect to electric field and higher proportion of added fibroblasts demanded a higher stimulation threshold [15•]. All of these properties reflect the characteristics of a well-insulated endogenous cardiac pacemaker tissue, such as the SA node [16]. These properties are consistent with the previously reported disorganized cellular orientation of the SA node consisting of weak cell-to-cell electrical coupling [1]. In line with the previous findings, 3D spheroids consisting of TBX18-iPMs raised the strength-duration threshold (Fig. 1A), reinforcing the electrical and morphological hallmarks the iPMs share with the native pacemaker cells. TBX18-iPMs, similar to native pacemaker cells, exhibited a more depolarized maximum diastolic potential, further contributing to the higher required external stimulation threshold [15•].The properties delineated above suggest that an ideal, electrically insulated cardiac tissue structure should be small in size, containing non-myocytes such as fibroblasts and isotropic in the core. These elements would intrinsically protect the pacemaker tissue from hyperpolarizing events from the neighboring myocardium.

TBX18-iPMs Are Resistant to Hypoxic Stress

Earlier studies have observed that the isolated, native SA node is able to withstand and recover from severe hypoxia compared with the myocardium [17, 18]. TBX18-iPMs were tested to determine whether they shared this ability and to provide a finer understanding of the adaptations needed to withstand metabolic stress. TBX18-iPMs exhibited negligible cell death after 2 days of near anoxia and/or inhibition of glycolysis, displaying lower oxygen consumption rates (OCRs), glycogen content, and secreted lactate concentration compared with those of ventricular myocytes [19•]. This indicates that the degree of oxidative phosphorylation and overall global metabolic demand are significantly lower in pacemaker myocytes compared with those in the chamber cardiomyocytes.

These results prompted evaluation of mitochondrial morphology within TBX18-iPMs, as mitochondria undergo dynamic fusion and fission processes in response to energetic need and stress [20, 21]. Transmission electron microscopy (TEM) of the iPMs revealed small, globular, and irregularly shaped mitochondria with sparse, disorganized cristae compared with that of the control GFP-NRVMs (Fig. 1B, C). Similar morphological patterns were observed in freshly isolated pacemaker cells from the SAN relative to the chamber cardiomyocytes from the same heart, an indication that both the native and induced pacemaker-like cells share a higher activity in mitochondrial fission than fusion processes [19•]. This notion was further supported by proteomic analysis of TBX18-iPMs and GFP-NRVMs which revealed downregulation of proteins that are associated with mitochondrial fusion (Mfn1, Mfn2, Opa1, Oma1, and Yme111) [21]. Knockdown with siRNA constructs against Opa1, one of the downregulated fusion proteins in TBX18-iPMs, was performed to facilitate fission in TBX18-iPMs. As a result, mitochondrial size and density were further reduced compared with those in TBX18-iPMs transfected with control siRNA. Monolayers of iPMs plated on multielectrode arrays (MEAs) recorded significantly increased synchronous pacing without a change in conduction velocity or gap junction protein levels [19•]. This suggests that mitochondrial fission directly facilitates the synchronous pacing of the iPMs without affecting the electrical coupling of the pacemaker cells.

Functionally, the apparent lower energy demand of TBX18-iPMs is conducive to the globular mitochondrial morphology. Compared with tubular morphology, globular mitochondria are known to be less efficient in generating ATP but more effective in eliminating damaged mitochondria upon stress [19•, 22, 23]. Thus, it appears that pacemaker myocytes are designed to maximize their survival at the expense of decreased ATP output. This allows for prioritization of generating spontaneous and oscillatory membrane depolarization under metabolic challenges.

TBX18 Tissue Constructs as a Model to Study the Ability of the SAN to Overcome Source-Sink Mismatch

The myocardium is electrically quiescent due to a significant electrical load provided by an inwardly rectifying K+ current, I_{K1} [24]. For the native SAN to initiate the heartbeat faithfully, the miniscule SAN needs to overcome the large electrical sink

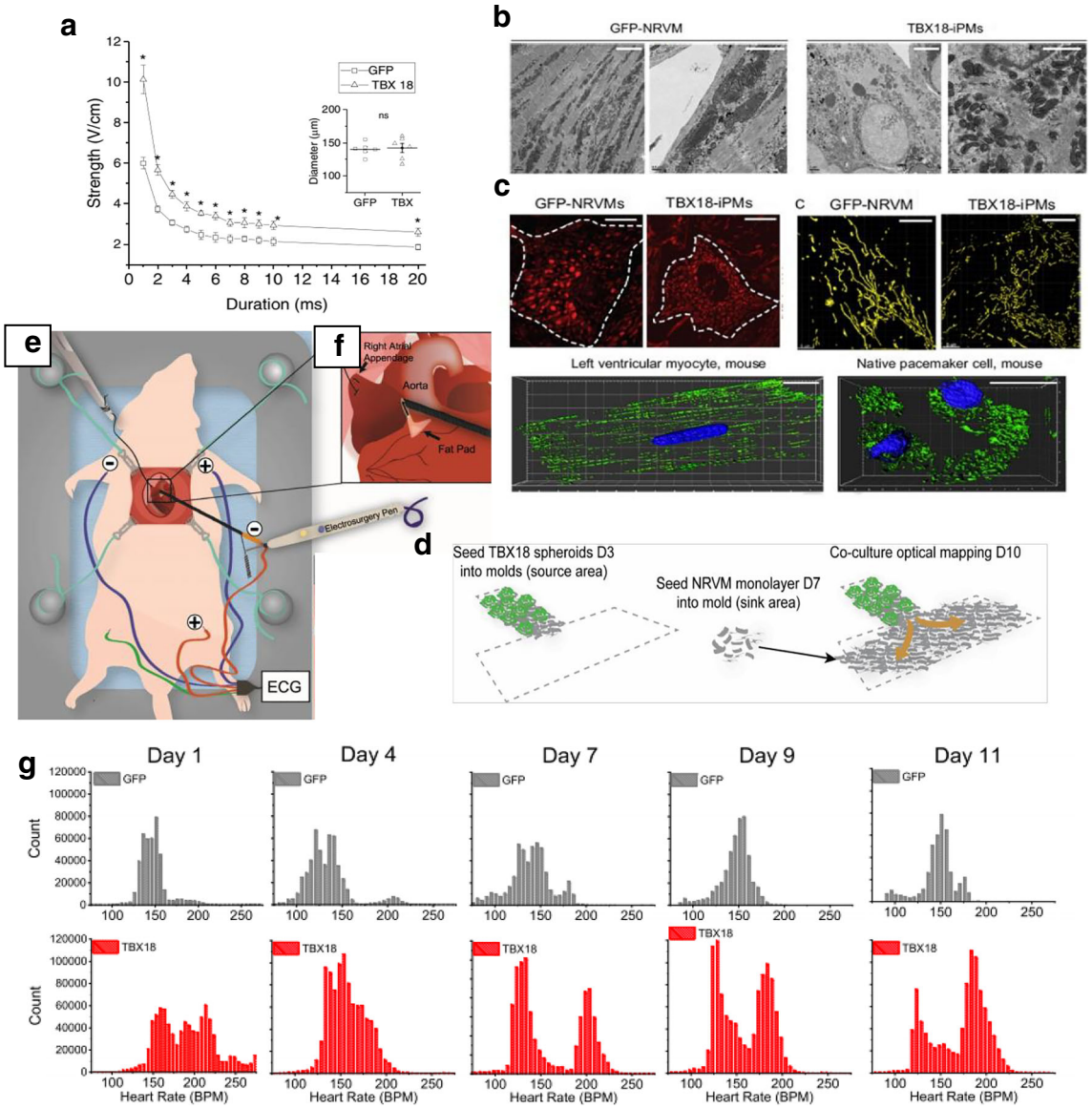

Fig. 1 A Strength-duration curve for diameter-matched GFP control vs TBX18 spheroids under I Hz electrical field stimulation, $n = 6$ per group. (Republished with permission from the American Physiological Society, from Sayegh MN, et al. *Am J Physiol Heart Circ Physiol*. 2019;317(1):H13–H25. doi:https://doi.org/10.1152/ajpheart.00161.2019; permission conveyed through Copyright Clearance Center, Inc.) [15•]. B EM images for GFP-NRVMs and TBX19-iPMs. C (*top*) Mitochondrial size distribution of GFP-NRVMs and TBX18-iPM. C (*bottom*) Superresolution images of mitochondria stained with MitoTracker from GFP-NRVMs and TBX18-iPMs. Scale bar 2 μm (B: *right panels*), 5 μm (B: *left panels*, C: *top*), and 10 μm (C: *bottom*). (Reproduced from: Gu J-m, et al. *Experimental & Molecular Medicine*. 2019;51(9):105. doi:https://doi.org/10.1038/s12276-019-0303-6; Creative Commons user license https://creativecommons.org/licenses/by/4.0/) [19•]. D Schematic of co-culture optical mapping (Reproduced from: Grijalva SI, et al. *Adv Sci* (Weinh). 2019 Sep 30;6(22):1901099. doi: https://doi.org/10.1002/advs.201901099; Creative Commons user license https://creativecommons.org/licenses/by/4.0/) [30•]. E Ablation needle, ECG electrodes, and electrosurgical pen contact site during CAVB procedure. F Needle entry is through the fat pad, pointing toward the LV apex. G Heart rate histograms of TBX18-injected rats show a second major peak 7 days post-gene delivery that is faster than the junctional rhythm (Republished with permission of Nature Publishing Group, from Kim NK, et al. *Scientific Reports*. 2019;9(1):6930. doi: https://doi.org/10.1038/s41598-019-43,300-9, permission conveyed through Copyright Clearance Center, Inc.) [36•]

in the atrial myocardium [25]. Once the SAN succeeds in pacing-and-driving the atrial myocardium, antegrade propagation is achieved via a ventricular conduction system. Key structural and electrical SAN design elements have been understood to facilitate the initiation of the heartbeat [26, 27]. These elements include weak electrical coupling of the pacemaker cells in the core of the SAN, and the anisotropic organization of pacemaker cells in contrast to the well-oriented myocytes in the myocardium. In addition, a transitional region between the SAN and the neighboring atrial myocardium appear to consist of hybrid cells with atrial myocyte morphology and pacemaker cell automaticity [25, 28, 29].

As a first approximation of the SAN's ability to overcome source-sink mismatch, we employed TBX18-iPMs as the source cells and monolayers of NRVMs as the electrical sink [30•]. To mimic the 3D architecture of the SAN and its weak electrical coupling at the core protecting the automaticity [25, 28, 31], we constructed spheroids consisting of either TBX19-iPMs or GFP-NRVMs (Fig. 1D).

TBX18-iPM spheroids (sphTBX18) showed low cell-cell electrical coupling, akin to the low electrical coupling within the native SAN. Expression of high conductance gap junctions, formed by Cx43, was significantly reduced in TBX18 spheroids and monolayers compared with that in control GFP spheroids (sphGFP) and GFP monolayers [30•]. The low Cx43 expression levels translated into slower conduction velocities in spheroids [30•] as well as monolayers [6] of TBX18-iPMs compared with controls.

When TBX18-iPM spheroids were seeded on a bed of NRVM monolayers, the co-culture showed faster syncytial automaticity compared with co-cultures consisting of GFP spheroids and NRVM monolayers. The syncytial automaticity from TBX18-iPM spheroids revealed a slower spike slope compared with that from control sphGFP. This is in line with the slow upstroke velocity of the SAN pacemaker action potentials due to minimal expression of I_{Na}. Interestingly, the rate of spontaneous and syncytial automaticity was faster in sphTBX18 co-cultured with NRVM monolayers compared with that in sphTBX18 alone. This is unexpected since hyperpolarizing electronic influence from the NRVM monolayers would diminish the depolarizing current from the iPMs. We speculate that the NRVMs and/or the nominal non-myocytes in the NRVM may directly or indirectly enhance the syncytial pacing of TBX18-iPMs, a notion that warrants further investigation.

To better understand whether the faster pacing originated from TBX18 spheroids, we designated constructs which juxtaposed sphTBX18, the electrical "source," with monolayers of NRVMs, the electrical "sink," limiting the contact between sphTBX18 and NRVMs to one side. Optical mapping of Ca^{2+} wave propagations demonstrated that the pacing originated from sphTBX18 and propagated out into the NRVM monolayer sink (Fig. 1D). In sphGFP, spontaneous Ca^{2+} waves mostly arose from the corners of the NRVM monolayer, resembling reentrant arrhythmias. The frequency of source-to-sink propagation was higher when TBX18-iPM spheroids were surrounded on one side rather than when they were surrounded fully or when the area of the sink was larger. β-Adrenergic stimulation further increased the frequency of sphTBX18's pace-and-drive [7]. Thus, our data indicates that TBX18-iPMs successfully serve as a model of how the SAN overcomes the source-sink mismatch. Building on this platform, key structural and functional design elements of SAN to be tested include the shape of the source, isotropy/anisotropy in cellular orientation, a discrete exit pathway between the node and the myocardium, and the minimum pacemaker cell number required to pace-and-drive a given electrical load.

Rodent Model of Complete Atrioventricular Block with Clinical Indices of Severe Bradyarrhythmias

Therapeutic potential of biological pacemakers needs to be tested in an animal model of severe bradycardia. We had previously developed a porcine model of complete heart block [32]. Using this model, we and others have demonstrated that TBX18 could provide ventricular pacing at rates faster than the large animals' slow junctional rhythm [8, 33]. The large animal models, while the most appropriate for studies that precede clinical translation, are cost-prohibitive for early-stage development. Previous small animal models of bradyarrhythmia relied on transient dissociation of A-V synchrony by pharmacological cholinergic suppression [7, 34, 35]. We sought to create a rodent model of CAVB so that the disease-modifying activity of biological pacemakers could be studied longitudinally. We achieved this by ablating the AV junctional region of the rat heart via a partial thoracotomy (Fig. 1E, f). Guided by real-time recording of the subepicardial electrogram, delivery of a high-frequency electrical energy via a sharp needle could ablate and necrotize the target atrioventricular nodal (AVN) tissue and successfully captured clinical indices of chronic and severe bradyarrhythmia such as the structural remodeling and arrhythmogenicity [36•].

Severe ventricular bradycardia is known to trigger compensatory remodeling and increased arrhythmogenicity [11, 37, 38], phenomena that were recapitulated in the CAVB rats. CAVB rats showed an increase in premature ventricular contractions (PVCs), skipped beats, and/or non-sustained ventricular tachyarrhythmias in the first few days post op. By 1-week post-surgery, these rhythm abnormalities had subsided. Instead, by 4 weeks, the majority of CAVB animals displayed higher arrhythmia inducibility such as sustained and non-sustained ventricular tachycardias or ventricular fibrillation upon programmed electrical stimulation compared with sham-operated ones [36•]. Hemodynamic remodeling due to the severe bradycardia included an immediate increase in stroke volume, likely to compensate for reduced cardiac output [4], followed by structural remodeling of the left ventricle over 4 weeks. Specifically, end-diastolic and end-systolic volumes, diastolic left ventricular internal diameter, and left ventricular stroke volume increased at the 4-week echocardiogram compared with those at baseline echo taken before the surgery.

Focal delivery of adenoviral TBX18 into the apex of the left ventricular myocardium 1 week after creating of the CAVB was preformed to test the efficacy of this gene-based

cardiac pacing. By day 7 post-gene delivery, a ventricular rate of > 200 bpm emerged in TBX18-injected animals [36•]. Beat-beat heart rate histograms, as seen in Fig. 1G, illustrate a bimodal distribution of heart rates in TBX18 animals, indicative of two competing pacing sites: one a slow junctional rhythm and the other a faster ectopic ventricular rate.

Taken together, the rat model of chronic CAVB is conducive to gaining mechanistic insight into ventricular modalities for mitigating the disease manifestation and the effectiveness of therapeutic options. Particularly, future studies on biological pacemakers can quantitatively asses their robustness, longevity, autonomic regulation, and arrhythmogenic risks with this ambulatory rat model.

Conclusions

These studies highlight the intricacies of cardiac pacing and delineate design considerations for future iterations of biological pacemakers. First, electrical conduction studies outline the physiologic parameters that provide native pacemaker nodal structures the protection from extra-nodal hyperpolarizing potentials in the heart [15•]. Metabolic studies of SAN hypoxic resistance reinforce our understanding and highlight distinctions in metabolism and mitochondrial morphology that seem to positively correlate with synchronous automaticity of iPMs [19•]. These characterizations should also be considered within physiologically based design principles for successful pace-and-drive function. These include weak cell-cell electrical coupling, electrical insulation of the SAN by non-myocytes, regions of isotropic and anisotropic cell alignment, and a discreet exit pathway from the SAN out to the atrial myocardium.

Further iterations of this somatic reprogramming system will be complemented by a deeper understanding of complete heart block progression provided by a novel, easily reproducible rat model [36•]. Our small animal model that properly reflects the clinical indices of bradycardia will accelerate understanding of disease evolution and pathophysiology and guide the development of therapeutic strategies. Future studies need to address the apparent waning of TBX18-induced biological pacemaker activity by week 2 after gene transfer in the porcine model [8, 33] so as to achieve the durability of biological pacing. To increase safety profiles for eventual clinical translation, especially in the pediatric population, development of non-viral gene transfer methods is warranted.

Compliance with Ethical Standards

Conflict of Interest Angel Xiao declares no conflict of interest. Hee Cheol Cho has a patent US Patent Number 14/357,195 issued.

Human and Animal Rights and Informed Consent This article does not contain any studies with human or animal subjects performed by any of the authors.

References

Papers of particular interest, published recently, have been highlighted as:
- • Of importance
- •• Of major importance

1. Bleeker WK, Mackaay AJ, Masson-Pevet M, Bouman LN, Becker AE. Functional and morphological organization of the rabbit sinus node. Circ Res. 1980;46(1):11–22. https://doi.org/10.1161/01.res.46.1.11.
2. Cho HC, Marban E. Biological therapies for cardiac arrhythmias: can genes and cells replace drugs and devices? Circ Res. 2010;106(4):674–85. https://doi.org/10.1161/circresaha.109.212936.
3. Tracy CM, Epstein AE, Darbar D, DiMarco JP, Dunbar SB, Estes NA 3rd, et al. 2012 ACCF/AHA/HRS focused update of the 2008 guidelines for device-based therapy of cardiac rhythm abnormalities: a report of the American College of Cardiology Foundation/American Heart Association Task Force on Practice Guidelines. J Thorac Cardiovasc Surg. 2012;144(6):e127–45. https://doi.org/10.1016/j.jtcvs.2012.08.032.
4. Bordachar P, Zachary W, Ploux S, Labrousse L, Haissaguerre M, Thambo J-B. Pathophysiology, clinical course, and management of congenital complete atrioventricular block. Heart Rhythm. 2013;10(5):760–6. https://doi.org/10.1016/j.hrthm.2012.12.030.
5. Cho HC. Pacing the heart with genes: recent progress in biological pacing. Curr Cardiol Rep. 2015;17(8):65. https://doi.org/10.1007/s11886-015-0620-x.
6. Kapoor N, Galang G, Marban E, Cho HC. Transcriptional suppression of connexin43 by TBX18 undermines cell-cell electrical coupling in postnatal cardiomyocytes. J Biol Chem. 2011;286(16):14073–9. https://doi.org/10.1074/jbc.M110.185298.
7. Kapoor N, Liang W, Marban E, Cho HC. Direct conversion of quiescent cardiomyocytes to pacemaker cells by expression of Tbx18. Nat Biotechnol. 2013;31(1):54–62. https://doi.org/10.1038/nbt.2465.
8. Hu Y-F, Dawkins JF, Cho HC, Marbán E, Cingolani E. Biological pacemaker created by minimally invasive somatic reprogramming in pigs with complete heart block. Sci Transl Med. 2014;6(245):245ra94. https://doi.org/10.1126/scitranslmed.3008681.
9. Oros A, Beekman JDM, Vos MA. The canine model with chronic, complete atrio-ventricular block. Pharmacol Ther. 2008;119(2):168–78. https://doi.org/10.1016/j.pharmthera.2008.03.006.
10. Piron J, Quang KL, Briec F, Amirault J-C, Leoni A-L, Desigaux L, et al. Biological pacemaker engineered by nonviral gene transfer in a mouse model of complete atrioventricular block. Mol Ther. 2008;16(12):1937–43. https://doi.org/10.1038/mt.2008.209.
11. Le Quang K, Benito B, Naud P, Qi Xiao Y, Shi Yan F, Tardif J-C, et al. T-type calcium current contributes to escape automaticity and governs the occurrence of lethal arrhythmias after atrioventricular block in mice. Circ Arrhythm Electrophysiol. 2013;6(4):799–808. https://doi.org/10.1161/CIRCEP.113.000407.
12. Park J, Ryu J, Choi SK, Seo E, Cha JM, Ryu S, et al. Real-time measurement of the contractile forces of self-organized cardiomyocytes on hybrid biopolymer microcantilevers. Anal Chem. 2005;77(20):6571–80. https://doi.org/10.1021/ac0507800.

13. Plonsey R, Barr RC. Bioelectricity: a quantitative approach. Boston: Springer; 2007.
14. Tung L, Sliz N, Mulligan MR. Influence of electrical axis of stimulation on excitation of cardiac muscle cells. Circ Res. 1991;69(3):722–30. https://doi.org/10.1161/01.RES.69.3.722.
15.• Sayegh MN, Fernandez N, Cho HC. Strength-duration relationship as a tool to prioritize cardiac tissue properties that govern electrical excitability. Am J Physiol Heart Circ Physiol. 2019;317(1):H13–25. https://doi.org/10.1152/ajpheart.00161.2019 **This experiment defined the strength-duration relationship as a metric of pacemaker function.**
16. Radisic M, Park H, Shing H, Consi T, Schoen FJ, Langer R, et al. Functional assembly of engineered myocardium by electrical stimulation of cardiac myocytes cultured on scaffolds. Proc Natl Acad Sci. 2004;101(52):18129–34. https://doi.org/10.1073/pnas.0407817101.
17. Kohlhardt M, Mnich Z, Maier G. Alterations of the excitation process of the sinoatrial pacemaker cell in the presence of anoxia and metabolic inhibitors. J Mol Cell Cardiol. 1977;9(6):477–88. https://doi.org/10.1016/S0022-2828(77)80027-8.
18. Nishi K, Yoshikawa Y, Sugahara K, Morioka T. Changes in electrical activity and ultrastructure of sinoatrial nodal cells of the rabbit's heart exposed to hypoxic solution. Circ Res. 1980;46(2):201–13. https://doi.org/10.1161/01.RES.46.2.201.
19.• Gu J-M, Grijalva SI, Fernandez N, Kim E, Foster DB, Cho HC. Induced cardiac pacemaker cells survive metabolic stress owing to their low metabolic demand. Exp Mol Med. 2019;51(9):105. https://doi.org/10.1038/s12276-019-0303-6 **These experiments defined the metabolic profile of induced pacemaker cells.**
20. Parra V, Verdejo H, del Campo A, Pennanen C, Kuzmicic J, Iglewski M, et al. The complex interplay between mitochondrial dynamics and cardiac metabolism. J Bioenerg Biomembr. 2011;43(1):47–51. https://doi.org/10.1007/s10863-011-9332-0.
21. Youle RJ, van der Bliek AM. Mitochondrial fission, fusion, and stress. Science. 2012;337(6098):1062–5. https://doi.org/10.1126/science.1219855.
22. Cogliati S, Enriquez JA, Scorrano L. Mitochondrial cristae: where beauty meets functionality. Trends Biochem Sci. 2016;41(3):261–73. https://doi.org/10.1016/j.tibs.2016.01.001.
23. Gottlieb RA, Bernstein D. Mitochondrial remodeling: rearranging, recycling, and reprogramming. Cell Calcium. 2016;60(2):88–101. https://doi.org/10.1016/j.ceca.2016.04.006.
24. Anumonwo JMB, Lopatin AN. Cardiac strong inward rectifier potassium channels. J Mol Cell Cardiol. 2010;48(1):45–54. https://doi.org/10.1016/j.yjmcc.2009.08.013.
25. Unudurthi SD, Wolf RM, Hund TJ. Role of sinoatrial node architecture in maintaining a balanced source-sink relationship and synchronous cardiac pacemaking. Front Physiol. 2014;5:446. https://doi.org/10.3389/fphys.2014.00446.
26. Noble D. A modification of the Hodgkin—Huxley equations applicable to Purkinje fibre action and pacemaker potentials. J Physiol. 1962;160(2):317–52. https://doi.org/10.1113/jphysiol.1962.sp006849.
27. Trenor B, Cardona K, Saiz J, Noble D, Giles W. Cardiac action potential repolarization revisited: early repolarization shows all-or-none behaviour. J Physiol. 2017;595(21):6599–612. https://doi.org/10.1113/JP273651.
28. Joyner RW, Wilders R, Wagner MB. Propagation of pacemaker activity. Med Biol Eng Comput. 2007;45(2):177–87. https://doi.org/10.1007/s11517-006-0102-9.
29. Rohr S, Kucera JP, Fast VG, Kléber AG. Paradoxical improvement of impulse conduction in cardiac tissue by partial cellular uncoupling. Science. 1997;275(5301):841–4.
30.• Grijalva SI, Gu J-M, Li J, Fernandez N, Fan J, Sung Jung H, et al. Engineered cardiac pacemaker nodes created by TBX18 gene transfer overcome source-sink mismatch. Adv Sci (Weinh). 2019;6(22):1901099. https://doi.org/10.1002/advs.201901099 **This paper presented constructs that recapituate the in silico parameters needed to overcome source-sink mismatch in a tissue model.**
31. Bouman LN, Duivenvoorden JJ, Bukauskas FF, Jongsma HJ. Anisotropy of electrotonus in the sinoatrial node of the rabbit heart. J Mol Cell Cardiol. 1989;21(4):407–18. https://doi.org/10.1016/0022-2828(89)90651-2.
32. Cingolani E, Yee K, Shehata M, Chugh SS, Marbán E, Cho HC. Biological pacemaker created by percutaneous gene delivery via venous catheters in a porcine model of complete heart block. Heart Rhythm. 2012;9(8):1310–8. https://doi.org/10.1016/j.hrthm.2012.04.020.
33. Dawkins JF, Hu Y-F, Valle J, Sanchez L, Zheng Y, Marbán E, et al. Antegrade conduction rescues right ventricular pacing-induced cardiomyopathy in complete heart block. J Am Coll Cardiol. 2019;73(13):1673–87. https://doi.org/10.1016/j.jacc.2018.12.086.
34. Protze SI, Liu J, Nussinovitch U, Ohana L, Backx PH, Gepstein L, et al. Sinoatrial node cardiomyocytes derived from human pluripotent cells function as a biological pacemaker. Nat Biotechnol. 2016;35:56. https://doi.org/10.1038/nbt.3745 https://www.nature.com/articles/nbt.3745#supplementary-information. Accessed 12 Dec 2016
35. Boink GJJ, Robinson RB. Gene therapy for restoring heart rhythm. J Cardiovasc Pharmacol Ther. 2014;19(5):426–38. https://doi.org/10.1177/1074248414528575.
36.• Kim NK, Wolfson D, Fernandez N, Shin M, Cho HC. A rat model of complete atrioventricular block recapitulates clinical indices of bradycardia and provides a platform to test disease-modifying therapies. Sci Rep. 2019;9(1):6930. https://doi.org/10.1038/s41598-019-43300-9 **The paper was built upon previous in silico, in vitro, and animal models and established a rodent CAVD model.**
37. Bignolais O, Quang KL, Naud P, El Harchi A, Briec F, Piron J, et al. Early ion-channel remodeling and arrhythmias precede hypertrophy in a mouse model of complete atrioventricular block. J Mol Cell Cardiol. 2011;51(5):713–21. https://doi.org/10.1016/j.yjmcc.2011.07.008.
38. Bernstein BS, Silver ES, Liberman L. QT prolongation and torsades de pointes in a patient with heart block and a pacemaker. Cardiol Young. 2016;26(1):161–3. https://doi.org/10.1017/S1047951114002674.